

Characterization of Mn-modified $\text{Pb}(\text{Mg}_{1/3}\text{Nb}_{2/3})\text{O}_3\text{-PbZrO}_3\text{-PbTiO}_3$ single crystals for high power broad bandwidth transducers

Shujun Zhang,^{1,a)} Sung-Min Lee,² Dong-Ho Kim,² Ho-Yong Lee,^{1,2} and Thomas R. Shrout¹

¹Materials Research Institute, Pennsylvania State University, University Park, Pennsylvania 16802, USA

²Ceracomp Co., Ltd., Asan, Chungnam 330-816, Republic of Korea

(Received 13 August 2008; accepted 10 September 2008; published online 26 September 2008)

The effect of MnO_2 addition on the dielectric and piezoelectric properties of $0.4\text{Pb}(\text{Mg}_{1/3}\text{Nb}_{2/3})\text{O}_3\text{-}0.25\text{PbZrO}_3\text{-}0.35\text{PbTiO}_3$ single crystals was investigated. Analogous to acceptor doping in “hard” $\text{Pb}(\text{Zr},\text{Ti})\text{O}_3$ based polycrystalline materials, the Mn doped crystals exhibited enhanced mechanical Q (~ 1050) with low dielectric loss ($\sim 0.2\%$), while maintaining ultrahigh electromechanical coupling $k_{33} > 90\%$, inherent in domain engineered single crystals. The effect of acceptor doping was also evident in the build-up of an internal bias ($E_i \sim 1.6$ kV/cm), shown by a horizontal offset in the polarization-field behavior. Together with the relatively high usage temperature ($T_{R-T} \sim 140$ °C), the Mn doped crystals are promising candidates for high power and broad bandwidth transducers. © 2008 American Institute of Physics.

[DOI: 10.1063/1.2992081]

High power ultrasonic transducers generally use “hard” piezoelectric ceramics $\text{Pb}(\text{Zr},\text{Ti})\text{O}_3$ (PZT), including PZT4 and PZT8 (DOD types I and III)¹. These materials are characterized by low dielectric ($\tan \delta$) and mechanical losses (high mechanical quality factor Q). In general, to achieve the “hardening” effect, these materials are acceptor doped, e.g., $\text{Fe}^{3+}, \text{Mn}^{3+}, \text{Mn}^{4+}$ substitution for $\text{Zr}^{4+}/\text{Ti}^{4+}$, resulting in the development of acceptor-oxygen vacancy defect dipoles. These dipoles align parallel to the polarization direction, leading to an internal bias, as evident in a horizontal offset in the polarization-electric field (P - E) behavior. This offset effectively increases the coercive field (E_C) and reduces or clamps domain wall motion/mobility.^{2,3} A consequence of these dopants, however, is a reduction in electromechanical coupling and piezoelectric activity, with k_{33} values less than 70% and piezoelectric strain coefficients d_{33} 's on the order of 200–350 pC/N,⁴ so limits the bandwidth of transducer since the power and bandwidth capabilities of the transducer are functions of the mechanical quality and electromechanical coupling factors^{5,6}. Recently, domain engineered $\langle 001 \rangle$ oriented single crystal perovskites have been demonstrated to possess ultrahigh electromechanical couplings $k_{33} > 90\%$ and high piezoelectric coefficients $d_{33} > 1500$ pC/N. However, the relaxor- PbTiO_3 (PT) crystals exhibit low mechanical quality Q 's (< 100) and coercive fields ($E_C \sim 2\text{--}3$ kV/cm), typical of “soft” piezoelectric behavior.^{7–9} Numerous efforts have been made to piezoelectrically harden the crystals through the addition of acceptor dopants. To date, only moderate mechanical Q values in the range of 200–300 have been achieved in flux grown $\text{Pb}(\text{Zn}_{1/3}\text{Nb}_{2/3})\text{O}_3\text{-PbTiO}_3$ crystals.^{10–12}

In this work, the effect of acceptor doping with MnO_2 in solid state crystal grown (SSCG) $0.4\text{Pb}(\text{Mg}_{1/3}\text{Nb}_{2/3})\text{O}_3\text{-}0.25\text{PbZrO}_3\text{-}0.35\text{PbTiO}_3$ (PMN-PZT) crystals was investigated. The SSCG method was se-

lected owing to its inherent benefit of maintaining dopant uniformity in a solid solution, unlike the melt Bridgman process. The PMN-PZT composition was selected owing to its relatively high coercive field ($E_C \sim 5$ kV/cm) and high temperature usage range ($T_{R-T} > 140$ °C).^{13–16}

Pure and manganese modified PMN-PZT single crystals were grown by the SSCG method. Sample geometries were determined for the full set of material constants measurement according to IEEE Standards.^{17–20} Prior to the measurements, the samples were poled and aged for 24 h. The Curie temperature T_C and ferroelectric phase transition temperature (T_{R-T}) were determined from the dielectric temperature dependence. High field measurements including polarization electric field hysteresis and strain loops were performed on $[001]$ oriented plate samples.

Figure 1 shows the dielectric behavior as a function of temperature for pure and modified PMN-PZT crystals. The Curie temperature T_C and rhombohedral to tetragonal phase transition temperature T_{R-T} were found to be on the order of 203 and 141 °C, respectively. For the Mn-modified PMN-PZT crystals, both transition temperatures were shifted

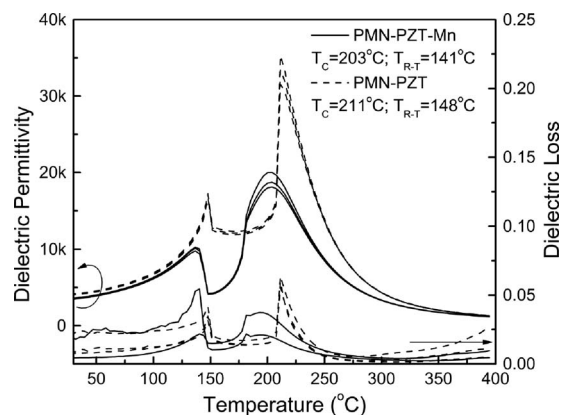


FIG. 1. Dielectric permittivity and dielectric loss as a function of temperature for pure and Mn modified PMN-PZT single crystals, measured at frequencies of 1 k–100 kHz.

^{a)}Author to whom correspondence should be addressed. Electronic mail: soz1@psu.edu.

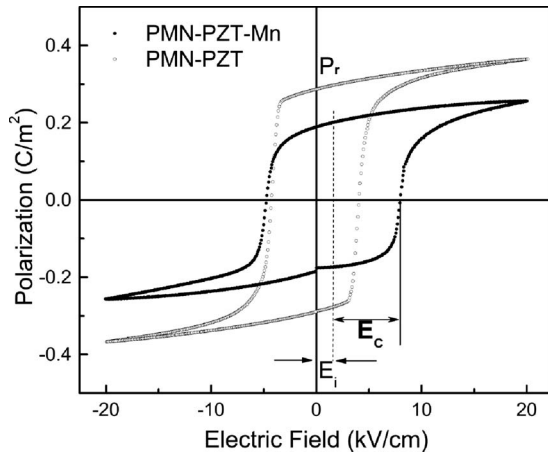


FIG. 2. Bipolar polarization hysteresis of pure and Mn modified PMN-PZT single crystals, measured at 20 kV/cm field.

downward a few degrees. The dielectric permittivity was found to be suppressed for the modified crystals due to domain wall pinning. As in acceptor doped hard PZT ceramics, $\text{Mn}^{3+,2+}$ cations are believed to be substituted into the $\text{Zr}^{4+}/\text{Ti}^{4+}$ sites, resulting in oxygen vacancies, leading to the development of acceptor-oxygen vacancy defect dipoles. Since there are no grain boundaries, the defect dipoles in hard PMN-PZT single crystals can occupy energetically preferred sites in the lattice, forming anisotropic centers, locally or within a domain. The dipoles thus align themselves along a preferential direction for the spontaneous polarization, and/or move to the high-stressed areas of domain walls by diffusion, pin the walls, and stabilize the domains.² The build-up of these parallel defect dipoles to the local polarization vector leads to an offset of P - E behavior or internal bias, as shown in Fig. 2, being on the order of 1.6 kV/cm, about one-fourth the level of the coercive field. The introduction of this internal bias effectively increases the E_C by 40% when compared to the undoped crystal, being ~ 6.3 kV/cm. The remnant polarization was found to be reduced from 0.29 to 0.18 C/m² for the modified PMN-PZT crystals, demonstrating that the degree of “switchable” polarization is significantly reduced, owing to domain clamping.

Figure 3 presents the unipolar strain curves (x - E) as a function of electric field for pure and modified crystals. As expected, low hysteresis (obtained by the ratio of $\Delta x/x$, as shown in Fig. 3), being on the order of 5%–6%, was observed for both crystals, similar to the value of hard PZT8 ceramics. The piezoelectric strain coefficients determined from the slope of x - E curve, resulted in d_{33} values of 1560 and 1170 pC/N for pure and modified crystals, respectively.

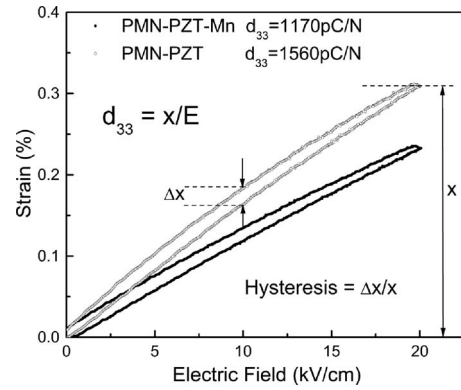


FIG. 3. Unipolar strain-electric field curves for pure and Mn modified PMN-PZT single crystals.

Table I lists characteristic properties for Mn modified PMN-PZT crystals as compared to undoped crystals and hard PZT ceramics. The coercive field and mechanical Q were found to increase and the dielectric loss decreased for the modified crystals, a consequence of the formation of internal bias and associated domain wall pinning, a particularly characteristic of hard piezoelectric materials. Although both the piezoelectric and dielectric properties decreased, the electromechanical coupling factor k_{33} remained greater than 90%, significantly higher than that of the hard PZTs ($\sim 70\%$).

For high power applications that require high piezoelectric properties and low loss (high mechanical quality factor), the figure of merit (FOM), product of Q and d , is an important factor to evaluate piezoelectric materials.⁴ As anticipated, the FOM of Mn modified PMN-PZT was found to be one order of magnitude higher than both the undoped crystal and hard PZT ceramics. Though there is no ferroelectric-ferroelectric phase transformation for PZT4 and PZT8 polycrystalline ceramics prior to their respective Curie temperatures, their usage temperature range is generally limited to less than half of the Curie temperature,²¹ which is on the same order of T_{R-T} of the crystals.

Table II lists the full set of material constants, including piezoelectric coefficients, electromechanical coupling factors, dielectric permittivities, elastic compliance and stiffness constants for both undoped and Mn-modified PMN-PZT crystals. As presented, the piezoelectric coefficients were found to decrease with doping, but the electromechanical coupling factors maintained similar values, demonstrating that the domain wall clamping has no effect on the coupling factors. The dielectric $\epsilon_{33}^T/\epsilon_0$ was found to decrease for Mn-modified crystals, while the dielectric $\epsilon_{11}^T/\epsilon_0$ increased, exhibiting less anisotropic behavior for the modified crystals

TABLE I. Application parameters of pure and Mn-modified PMN-PZT single crystals, compared to hard PZT ceramics.

| Material | T_C (°C) | T_{R-T} (°C) | P_r (C/m ²) | E_C (kV/cm) | E_i (kV/cm) | $\frac{\epsilon_{33}^T}{\epsilon_0}$ | Loss (%) | d_{33} (pC/N) | k_{33} | Q | FOM ^a (pC/N) |
|------------|---------------|-------------------|------------------------------|------------------|------------------|--------------------------------------|-------------|--------------------|----------|------|----------------------------|
| PMN-PZT | 211 | 148 | 0.29 | 4.5 | / | 4850 | 0.5 | 1530 | 0.93 | 100 | 1.5×10^5 |
| PMN-PZT-Mn | 203 | 141 | 0.18 | 6.3 | 1.6 | 3410 | 0.2 | 1140 | 0.92 | 1050 | 1.2×10^6 |
| PZT4 | 328 | ^b | 0.36 | 14.2 | 3.0 | 1300 | 0.4 | 300 | 0.70 | 500 | 1.5×10^5 |
| PZT8 | 300 | ^b | 0.26 | 18.7 | 7.0 | 1000 | 0.4 | 230 | 0.64 | 1000 | 2.3×10^5 |

^aFOM = Qd_{33} .

^bUsage temperature range of ferroelectric ceramic is limited by $\frac{1}{2}T_C$ (Ref. 21).

TABLE II. Measured and derived piezoelectric coefficients d_{ij} (pC/N), e_{ij} (C/m²), g_{ij} (10⁻³ Vm/N), h_{ij} (10⁸ V/m), Electromechanical coupling factors k_{ij} , dielectric permittivity ϵ_{ij} (ϵ_0), dielectric impermeability β_{ij} (10⁻⁴/ ϵ_0), elastic compliance constants s_{ij} (10⁻¹² m²/N), elastic stiffness constants c_{ij} (10¹⁰ N/m²), for pure and Mn-modified PMN-PZT crystals.

| Material | d_{33} | d_{31} | d_{15} | g_{33} | g_{31} | g_{15} | e_{33} | e_{31} | e_{15} | h_{33} | h_{31} | h_{15} |
|------------|------------|------------|------------|------------|-------------------|-------------------|-------------------|-------------------|----------------|----------------|----------------|----------------|
| PMN-PZT | 1530 | -718 | 133 | 35.6 | -16.7 | 21.6 | 17.7 | -7.4 | 7.5 | 34.0 | -14.1 | 14.5 |
| PMN-PZT-Mn | 1140 | -513 | 107 | 37.8 | -17.0 | 12.5 | 17.0 | -6.1 | 7.1 | 37.7 | -13.4 | 9.1 |
| Material | k_{33} | k_{31} | k_{15} | k_t | ϵ_{33}^T | ϵ_{11}^T | ϵ_{33}^S | ϵ_{11}^S | β_{33}^T | β_{11}^T | β_{33}^S | β_{11}^S |
| PMN-PZT | 0.93 | 0.44 | 0.40 | 0.60 | 4850 | 697 | 590 | 580 | 2.06 | 14.35 | 16.95 | 17.24 |
| PMN-PZT-Mn | 0.92 | 0.45 | 0.30 | 0.59 | 3410 | 970 | 510 | 880 | 2.93 | 10.31 | 19.61 | 11.36 |
| Material | s_{11}^E | s_{12}^E | s_{13}^E | s_{33}^E | s_{44}^E | s_{66}^E | s_{11}^D | s_{12}^D | s_{13}^D | s_{33}^D | s_{44}^D | s_{66}^D |
| PMN-PZT | 62.0 | -31.8 | -28.4 | 62.8 | 17.8 | 26.1 | 50.0 | -43.8 | -2.9 | 8.1 | 15.0 | 26.1 |
| PMN-PZT-Mn | 42.6 | -19.9 | -22.1 | 51.3 | 15.2 | 29.9 | 33.9 | -28.6 | -2.7 | 8.1 | 13.9 | 29.9 |
| Material | c_{11}^E | c_{12}^E | c_{13}^E | c_{33}^E | c_{44}^E | c_{66}^E | c_{11}^D | c_{12}^D | c_{13}^D | c_{33}^D | c_{44}^D | c_{66}^D |
| PMN-PZT | 11.7 | 10.6 | 10.1 | 10.7 | 5.6 | 3.8 | 12.7 | 11.6 | 7.6 | 16.7 | 6.7 | 3.8 |
| PMN-PZT-Mn | 14.3 | 12.7 | 11.7 | 12.0 | 6.6 | 3.3 | 15.2 | 13.6 | 9.4 | 18.4 | 7.2 | 3.3 |

when compared to the undoped crystals. Also from Table II, the elastic compliance constants were found to decrease with Mn doping, whereas the elastic stiffness constants increased, indicating a higher acoustic velocity when compared to the undoped counterpart.

Of particular interest is the “soft shear acoustic wave” that propagates along $\langle 110 \rangle$ with displacement along the $\langle 011 \rangle$ direction. Experimental results reported that domain wall motion results in a large effective $(s_{11}^E - s_{12}^E)$,¹⁸ with low soft shear acoustic velocity. From Table II, the value of $(s_{11}^E - s_{12}^E)$ was found to drop by 33% for the Mn-modified PMN-PZT crystals, from which the velocity was calculated to be on the order of 1000 m/s, higher than the value of pure crystals (~ 830 m/s), indicative of the reduced domain wall motion owing to the domain wall pinning by defect dipoles.

In summary, pure and Mn-modified PMN-PZT crystals were grown using the SSCG method. The modified crystals exhibited higher coercive field and Q , with reduced dielectric and piezoelectric properties, typical of hard behavior. The internal bias field in the Mn modified PMN-PZT crystal is believed to play an important role in the pinning and/or clamping of domain walls. The FOM Qd for the Mn modified PMN-PZT crystals was found to be one order of magnitude higher than both pure crystals and hard PZT ceramics. Together with its comparable temperature usage range and ultra high electromechanical coupling factor, make Mn-modified PMN-PZT crystals promising candidates for high power and broad bandwidth transducers.

This work was supported by the Office of Naval Research (ONR) and National Institutes of Health (NIH) under Grant No. P41-RR11795.

¹R. C. Pohanka and P. L. Smith, *Electronic Ceramics: Properties, Devices and Applications*, edited by L. M. Levinson (Marcel Dekker, New York, 1987), Chap. 2.

²K. Carl and K. H. Hardtl, *Ferroelectrics* **17**, 473 (1978).

³S. Takahashi, *Ferroelectrics* **41**, 143 (1982).

⁴S. J. Zhang, R. Xia, L. Lebrun, D. Anderson, and T. R. Shrout, *Mater. Lett.*, **59**, 3471 (2005).

⁵R. J. Meyer, T. C. Montgomery, and W. J. Hughes, *Oceans '02 MTS/IEEE Proceeding*, Mississippi, 29–31 October 2002 (unpublished), p. 2328.

⁶T. C. Montgomery, R. J. Meyer, and E. M. Bienert, *Oceans '07 MTS/IEEE Proceeding*, Vancouver, 29 September–4 October, 2007 (unpublished).

⁷S. E. Park and T. R. Shrout, *J. Appl. Phys.* **82**, 1804 (1997).

⁸S. J. Zhang, J. Luo, R. Xia, P. W. Rehrig, C. A. Randall, and T. R. Shrout, *Solid State Commun.* **137**, 16 (2006).

⁹D. Damjanovic, M. Budimir, M. Davis, and N. Setter, *J. Mater. Sci.* **41**, 65 (2006).

¹⁰S. Priya, H. W. Kim, J. Ryu, S. J. Zhang, T. R. Shrout, and K. Uchino, *J. Appl. Phys.* **92**, 3923 (2002).

¹¹S. J. Zhang, L. Lebrun, C. A. Randall, and T. R. Shrout, *J. Cryst. Growth* **267**, 204 (2004).

¹²D. Kobor, L. Lebrun, G. Sebald, and D. Guyomar, *J. Cryst. Growth* **275**, 580 (2005).

¹³S. J. Zhang, S. M. Lee, D. H. Kim, H. Y. Lee, and T. R. Shrout, *Appl. Phys. Lett.* **90**, 232911 (2007).

¹⁴A. Amin, H. Y. Lee, and B. Kelly, *Appl. Phys. Lett.* **90**, 242912 (2007).

¹⁵S. J. Zhang, S. M. Lee, D. H. Kim, H. Y. Lee, and T. R. Shrout, *J. Appl. Phys.* **102**, 114103 (2007).

¹⁶S. J. Zhang, S. M. Lee, D. H. Kim, H. Y. Lee, and T. R. Shrout, *J. Am. Ceram. Soc.* **90**, 3859 (2007).

¹⁷*IEEE Standard on Piezoelectricity* (ANSI/IEEE Standard, New York, 1987), p. 176.

¹⁸R. Zhang, B. Jiang, and W. Cao, *J. Appl. Phys.* **90**, 3471 (2001).

¹⁹S. J. Zhang, C. A. Randall, and T. R. Shrout, *J. Appl. Phys.* **95**, 4291 (2004).

²⁰X. C. Geng, T. A. Ritter, and S. E. Park, *Proc.-IEEE Ultrason. Symp.*, 571 (1998).

²¹T. R. Shrout, R. Eitel, and C. A. Randall, *Piezoelectric Materials in Devices*, edited by N. Setter (EPFL Swiss Federal Institute of Technology, Switzerland, 2002), p. 413.